Article

Joint Wear Prediction and Experiments Considering the Influences of Coating and Spherical Joint Clearances

Qian Jing [1,2,*] and Baolong Geng [1]

[1] School of Mechanical Engineering, Long Dong University, Qingyang 745000, China
[2] School of Mechanical and Precision Instrument Engineering, Xi'an University of Technology, Xi'an 710048, China
* Correspondence: jingq@ldxy.edu.cn; Tel.: +86-182-0934-6537

Abstract: In recent years, many scholars have carried out a large number of theoretical studies on mechanism systems with joint clearances. Some scholars have conducted relevant experiments with simple planar mechanisms, for example, which have proved the feasibility and applicability of the numerical dynamics calculation method and different contact force models to a certain extent. In order to verify the correctness of the theoretical analysis method of the system dynamics considering coating and joint clearances in the previous stage, this paper independently designed and built the RSSP experimental platform of the spatial four-bar mechanism by taking the shear fork mechanism of the soybean picking and separating machine in farming operations, and measured the dynamic changes in the execution components and the wear depth of the spherical shell surface in different working conditions. The effectiveness of the coating on alleviating vibration, reducing joint wear, and extending the working life of the system mechanism was verified. The experimental conclusions provide strong data support for the subsequent effective and long-life operation of the soybean picking and sorting integrated machine.

Keywords: coating; spherical joint clearance; dynamics; wear prediction; experiments

1. Introduction

Joint clearance is generated by the early processing accuracy and assembly requirements of various parts of the mechanical system and gradually increases after a long period of time. With the continuous improvement in agricultural machinery accuracy requirements, the impact of joint clearance on agricultural machinery can no longer be ignored. The constant increase in joint clearance size affects the mechanical characteristics of the adjacent components of the mechanism, thus creating negative effects, such as vibration, noise, wear, and heat, in the working process of the mechanism system; this also leads to a gradual decrease in the motion accuracy of the mechanism. Additionally, the dynamic performance deviates from what is expected, which ultimately affects the working efficiency and service life of the mechanism systems. Because joint clearances can seriously affect the dynamic behavior and reliability of mechanical systems, the mechanism becomes a nonlinear multi-degree-of-freedom system. Such nonlinearity seriously affects the motion accuracy of the actuator and the stability of the system, which requires high-precision motions [1]. The influence of joint clearances on the mechanism system mainly involves the following: (1) The joint clearances will inevitably cause the joint elements to have additional contact collisions during normal movement. Contact collision has a significant impact on the motion accuracy of the mechanism, especially the actuator. (2) The joint clearances will gradually increase with the extending operating time of the mechanism, and

the reduction in the motion accuracy and reliability of the mechanism will become more evident. (3) Between the dynamic pairs containing joint clearance, the joint wear generated by the contact collision force will further increase the size of joint clearance, and long-term operation will inevitably lead to a decrease in the motion precision and life expectancy of the mechanism. At present, the requirements for the stability and motion accuracy of mechanisms are increasing every year, especially in the fields of intelligent agricultural machinery, industrial robotics, and aerospace [2]. In mechanical operations, due to the low processing precision of mechanical parts and insufficient assembly precision, increased joint clearances of mechanical systems increase, while aggravated wear and tear, as well as declined productivity, also occur from time to time.

In recent years, many scholars have investigated different types of mechanisms containing space clearances based on the study of the planar clearance mechanism. Flores [3,4] modeled and simulated the space multi-body system, taking lubrication and spherical joint clearances into consideration, and analyzed the dynamic characteristics of the actuator of spherical joints with and without clearance lubrication, using the space crank slider mechanism (RSSR) as the example. Based on the preliminary research relating to the configuration synthesis, statics, and dynamics of the parallel mechanism, Wang [5] proposed a parallel mechanism with four degrees of freedom, which can achieve three rotations and one movement; Wang also analyzed in detail the influence of the parallel mechanism on its dynamic performance using numerical solution when considering spherical joint clearances. Also, with the parallel mechanism as their research object, Hou [6] adopted the Newton–Euler method to establish a dynamic model of the parallel mechanism (3-RSR) considering the spherical joint clearances, used the fourth-order Runge Kutta method to obtain the solution, and subsequently evaluated the simulation results. Tian [7] used the Reynolds equation to investigate the effects of fluid lubrication on the open-loop mechanism (double-pendulum) and the closed-loop mechanism (RSSR) containing spherical joint clearances and compared the results with the computational results obtained from the ADAMS software 2008. They proved that the introduction of fluid lubricant at the mechanism clearance joints can prevent the direct collision of the ball sockets. In [8,9], the authors compared and analyzed the slider dynamic results of the spatial slider crank mechanism (RSSP) in the presence of both axial and radial clearances when the axial dimensions of the rotating joints cannot be neglected in the following three different conditions: ideal joints, joints with frictionless clearance, and joints with friction clearance. Moreover, as concerns studies on the mechanisms containing spatial rotating joint clearances, with spatial double pendulums and circuit breakers as an example, Bai [10] and Narendra Akhadkar [11] adopted different numerical computation methods to compare and analyze the mechanism without clearances as well as the planar rotating joint mechanism and the spatial rotating joint mechanism. The results show that when both radial and axial clearances were considered for the three-dimensional rotating joints, the dynamic response of the mechanism with spatial motions was more unstable than that of the mechanism considering only radial clearances. For the spatial rotating joints, [12] the authors proposed a modified model for the contact force of 3D translational clearance joints to investigate the effect of oblique collisions and the geometrical changes in the contact region of double pendulums. The above studies involved in-depth theoretical research into the dynamic performance of different mechanism systems considering joint clearance, but most of them have not been verified by experiments.

Joint clearances may destroy the ideal model of the mechanism motion or increase the assembly clearances caused by the original assembly errors, as a result of which, the collision and vibration between the components will increase, which will have a significant impact on the dynamics performance of the mechanism [13,14]. At the same time, this effect will be exacerbated by wear and tear at the mechanism's clearance. However, because the

contact surface continuously changes with the increase in wear, higher requirements are placed on the calculation methods and accuracy of wear prediction. With a planar linkage mechanism as an example, Mukras S. [15] proposed a numerical modeling and design method to predict the vibrational wear of the contact body, which optimizes the wear prediction algorithm in terms of both computational cost and efficiency while guaranteeing computational accuracy. Based on their research, studies were carried out to investigate the effect of joint wear on the kinematics of a simple crank slider mechanism and the impact of the change in the mechanism kinematics on joint wear [16–18]. Based on the previous research on the collision problem of revolute joints with clearances, Flores [19] used the Achard wear model to quantify the pressure in the contact area and the wear caused by relative sliding by calculating the contact force, and proposed a wear prediction method for rotating joints with clearances. Wang [20–22] proposed an approximate calculation method for the contact area of spherical joints with clearances based on the multi-body system motion equation, and predicted the impact of wear-induced spherical joints with clearances on the dynamic performance of the spatial multi-body system. Zhuang [23] introduced a time-varying wear coefficient considering different lubrication conditions, simulated the wear of individual rotating joints by continuously updating the contact nodes, and verified the validity of the method in experiments evaluating the wear of rotating joints of the cabin door of an airplane. Feng [24] proposed a new method for calculating the wear depth taking into account the effect of Hertz deformation, and evaluated the effectiveness of the improved wear calculation method in gear wear prediction by carrying out durability experiments under two different lubrication conditions. Using a solar panel system as an example, Li [25] explored a multi-body system's dynamic response and wear characteristics considering joints with coating and clearances. A rigid–flexible coupling system was established based on the NCF–ANCF formula, in which NCF represents nodal coordinate formulation and ANCF represents absolute nodal coordinate formulation, and the clearance joint model was constructed based on the novel contact law considering coatings, the modified Coulomb Law of Friction and the Archard Wear Law. It is not difficult to see that the above wear prediction calculation is primarily based on the Archard wear model, mainly because the Archard wear model can be easily solved by normal contact force and slip distance. The model is a linear wear model, and the wear depth is highly convenient for the dynamic research based on the calculation of contact collision force using the continuous contact model.

Based on the above research status on the dynamics of clearance mechanism and contact force models considering coating and wear prediction methods, it can be seen that there is not much research on the dynamics of mechanism systems involving joint clearance, especially considering the coating as a method to reduce system vibration caused by clearance. Since the dynamics of the mechanism with joint clearance is affected by many factors, such as clearance value, driving speed, and number of clearances, most of the studies on joint clearance with rotating and spherical joints are only theoretical studies and lack relevant experimental verification. Considering that the experiment period of the coating on the vibration reduction and wear resistance of the mechanism system is long and the operation is complex, the method of variable driving speed and clearance value can be used to study the mechanism system dynamics. Therefore, with the scissors mechanism of the soybean picking and sorting machine as the prototype of our study, we mainly investigated the dynamics and joint wear of the spatial linkage mechanism considering the coating and the spherical joint clearances and validated the previous conclusions on the influence of spherical joint clearances on the dynamics of the mechanism through experiments, thus proving our conclusions on the wear prediction of spherical joint clearances considering coatings and the feasibility of our computation method. Our

experimental study can provide necessary data support for using coatings to improve the dynamic performance and productivity of the system of intelligent agricultural equipment. Our paper is organized as follows:

(i)   We introduce the background and significance of our study, mainly including the method of analyzing the dynamics of the mechanism containing spherical joint clearances, the current research on the effects of coatings in vibration reduction and abrasion resistance of the mechanism, as well as the commonly used methods of calculating the wear loss of joints containing clearances and the improvement measures.

(ii)   We describe the contact state determination method of the mechanism containing spherical joint clearances, inspired by the spherical joint contact collision force models and the spherical joint clearance wear calculation methods improved by considering the effect of coating properties and dimensions on variable stiffness coefficient in relevant works, and propose the dynamics model and wear prediction process for mechanism containing clearances used in our study.

(iii) With the soybean picking and sorting machine designed and developed by the Intelligent Agricultural Machinery Team as a carrier, we consider replacing the actuator of the soybean picking system with a spatial linkage mechanism, independently design and construct a spatial four-bar mechanism (RSSP) experimental platform, and introduce how to build the experimental platform and its structural composition.

(iv)   Using the constructed experimental platform and multiple test pieces (spherical joints), we measure the acceleration amplitude of the moving element and the wear depth of the inner surface of the shell under the same driving speed in different working conditions, compare the experimental data with the theoretical results, and validate the correctness of the previous analysis method and results.

(v)   The research content of this paper is summarized, and the innovation of the research conclusion is presented. The results of this paper provide a feasible and reliable theoretical basis for reducing system vibration and increasing the service life of intelligent agricultural equipment while considering joint clearances in the future.

2. Wear Prediction Containing Spherical Joint Clearances

2.1. Dynamics of Spherical Joints Containing Clearances

The purpose of the study is to analyze the dynamic characteristics of each component when the joint of the mechanism considers the clearance to provide a theoretical basis for the optimization of the structural parameters of the mechanism system that is more suitable for the actual working conditions, to ensure the stable performance of the mechanism system with the permitted accuracy and long life [26–28], and to provide a theoretical basis for the optimization of the structural parameters of the system that are more in line with the actual working conditions and ensure the stable performance and trouble-free, long-term operation of the system in the process of automation and intelligent operation.

Based on the kinematics and dynamics solution of mechanisms without clearance, the critical challenge in addressing the dynamics of mechanisms containing spherical joint clearances lies in accurately modeling the contact and collision process between the ball and the shell. The typical structure of spherical joints with clearances is illustrated in Figure 1. When clearances are present in spherical joints, the geometric centers of the moving shell i and sphere j do not coincide. *O-XYZ* denotes the global coordinate system, while $O_i - \xi_i\eta_i\zeta_i$ and $O_j - \xi_j\eta_j\zeta_j$ represent the local coordinate systems of shell i and sphere j, respectively. R_i and R_j denote shell i and sphere j radii, respectively. S_i^P and S_j^P represent the position vectors from the geometric centers of shell i and sphere j to their respective centers of mass in the local coordinate systems. r_i^P and r_j^P are the radial vectors of the geometric centers of shell i and sphere j in the global coordinate system, respectively; r_i

and r_j are the radial vectors of the centers of mass of the two components. According to the geometric relationship in Figure 1, it can be concluded that

$$\mathbf{r}_k^p = \mathbf{r}_k + \mathbf{A}_k S_k^p (k = i, j) \tag{1}$$

In the formula, $\mathbf{A}_k$ represents the coordinate transformation matrix of the local coordinates $O_k - \xi_k \eta_k \zeta_k$ relative to the global coordinates $O\text{-}XYZ$; then, the eccentricity vector $\mathbf{e}$ is as follows:

$$\mathbf{e} = \mathbf{r}_i^p - \mathbf{r}_j^p \tag{2}$$

The vector $\mathbf{n}$ in the collision direction between shell i and sphere j can be obtained through eccentricity:

$$\mathbf{n} = \frac{\mathbf{e}}{|\mathbf{e}|} \tag{3}$$
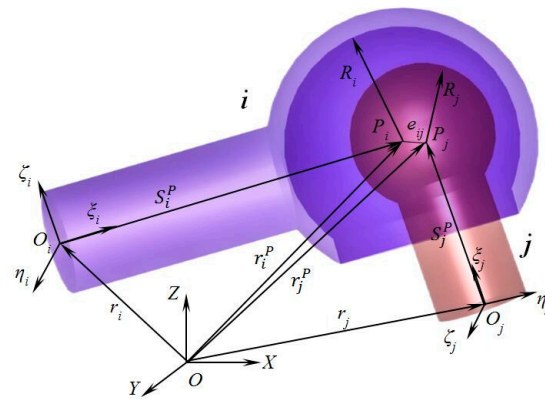
Figure 1. Spherical joint with clearance.

If θ_X, θ_Y, and θ_Z are used to represent the collision azimuths of the spherical joints containing clearances, and e_X, e_Y, and e_Z represent the eccentricities in various directions, that is, the angles and eccentricities between the normal direction of the contact element and the global coordinates X, Y and Z; the mathematical expression can be obtained from Figure 2.

$$\begin{cases} \theta_X = arccos \, \frac{e_X}{e} \\ \theta_Y = arccos \, \frac{e_Y}{e} \\ \theta_Z = arccos \, \frac{e_Z}{e} \end{cases} \tag{4}$$
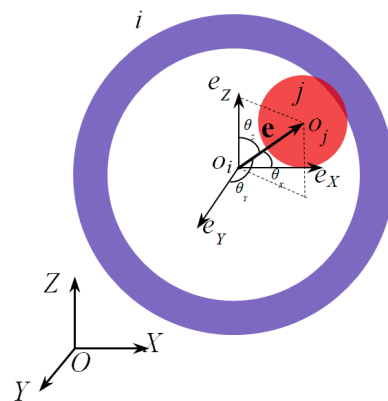
Figure 2. Impact azimuth of spherical joint with clearance.

According to the size of clearance c, the expression of the contact collision depth can be determined.

$$\delta = |\mathbf{e}| - c \tag{5}$$

The contact collision process of spherical joints containing clearances is described above. Figure 3 shows the three states during the contact collision process of spherical joints: Free motion, Critical contact, Contact and deformation. Based on relevant studies on the dynamics of mechanisms containing spherical joint clearances, our work adopts the Lagrange augmentation method to establish a mechanism dynamics model. The dynamic model of the mechanical system with joint clearance can be represented as follows [26]:

$$\begin{bmatrix} \mathbf{M} & \mathbf{C}_q^T \\ \mathbf{C}_q & 0 \end{bmatrix} \begin{bmatrix} \ddot{\mathbf{q}} \\ \lambda \end{bmatrix} = \begin{bmatrix} \mathbf{Q}_e + \sum_{i=1}^n \mathbf{F} \\ \gamma - 2\alpha\dot{\mathbf{C}} - \beta^2\mathbf{C} \end{bmatrix} \tag{6}$$
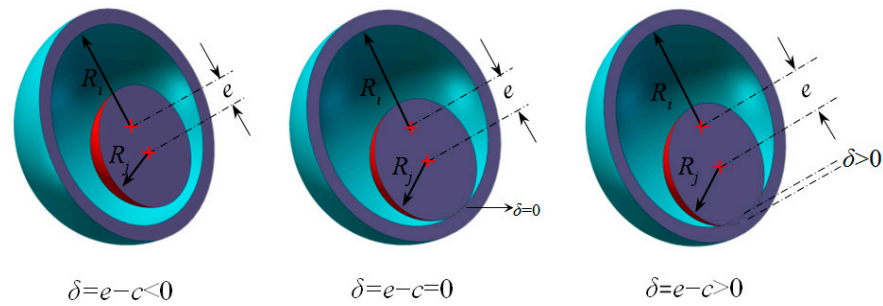

$\delta = e - c < 0$ $\delta = e - c = 0$ $\delta = e - c > 0$

Figure 3. Relative movement of the spherical joint with clearance.

In the coefficient matrix, M is the mass matrix of a rigid body; C is the constraint equation, and $\mathbf{C}_q$ is the Jacobian matrix of the mechanism. $\ddot{\mathbf{q}}$ is the acceleration vector of generalized coordinates, and λ is the Lagrange multiplier vector. On the right-hand side of the equation, $\mathbf{Q}_e$ is the generalized external force vector, $\sum_{i=1}^n \mathbf{F}$ is the sum of force vectors, and γ is the quadratic term of velocity. In this paper, the BAUMGARTE stabilization method [29] is employed to overcome the constraint violation in the equation.

Table 1 shows k_N represents the variable stiffness coefficient, and χ_N is the improved viscous damping coefficient. R_2 represents the inner radius of the spherical shell, and E_w^* represents the equivalent elastic modulus of the double elastic layer. α is a correction coefficient for the error caused by using the equivalent velocity to establish the dynamics equation, and c_r is the recovery coefficient of collision. ΔR represents the clearance between the spherical shell and the ball. In order to study the effect of coating materials on the dynamic properties of the spherical joint mechanism with clearance, the equivalent modulus of the double elastic layer contact force model was established.

Table 1. Improved normal contact force.

Contact Force	Variable Stiffness Coefficient	Viscous Damping Coefficient	Expression
F_c	$k_N = \frac{4\pi E_w^* R_2}{5} \frac{2\delta\Delta R + \delta^2}{(\Delta R + \delta)^2}$	$\chi_N = \frac{20k_N(1-c_r)}{13\alpha c_r \dot{\delta}^{(-)}}$	$F_c = k_N\delta^n + \chi_N\delta^n\dot{\delta}$

In order to study the influence of coating material on the dynamic performance of the mechanism containing spherical joint with clearance, the equivalent modulus of double elastic layers was established by using the method of establishing a contact force model with double elastic layers based on Winkler elastic foundation model and the hypothesis of elliptic pressure distribution in Hertz theory. The new variable stiffness coefficient of contact force is expressed in Table 1. Considering the influence of coating material and size on the stiffness coefficient, the equivalent elastic modulus of the double elastic layer is obtained as follows:

$$\frac{1}{E_w^*} = \frac{1 - v_i^2}{E_i^*} + \frac{1 - v_j^2}{E_j} \tag{7}$$

$$E_i^* = E_c^* E_s^* / (E_s^* l_c + E_c^* l_s) \tag{8}$$

$$E_{c,s}^* = \frac{E_{c,s}(1 - v_{c,s})}{(1 + v_{c,s})(1 - 2v_{c,s})} \tag{9}$$

where E_w^* represents the equivalent elastic modulus of the double elastic layer, E_c^*, and E_s^*, respectively, represent the equivalent elastic modulus of the coating and elastic modulus of the base, v_c and v_s, respectively, represent Poisson's ratio of the coating and base, and l_c and l_s represent the thickness of the layer and base in millimeters. R_1 and R_2 represent the ball's radius and the spherical shell's inner radius. The 3D physical model of the spherical joint with clearance and coating is shown in Figure 4a, and the contact model with a double elastic layer is shown in Figure 4b.
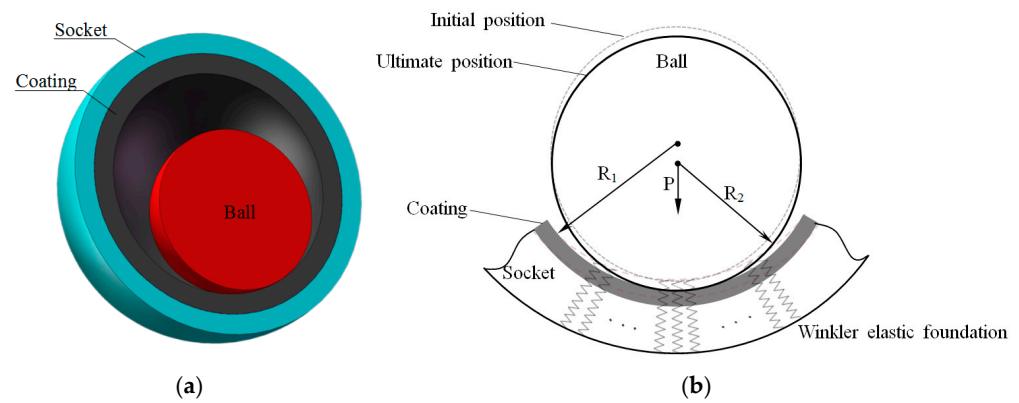

(**a**)   (**b**)

Figure 4. Double elastic layer contact model. (**a**) Physical model. (**b**) Geometrical model.

2.2. Wear Calculation of Spherical Joints Containing Clearances

Wear is a process in which the surface material is constantly damaged during the relative movement of the mechanical system contact components. When there is relative sliding between the surfaces of contact elements in the joints of a mechanical system, the surface material is lost or migrated due to the adhesive effect, that is, adhesive wear. The impact of wear-induced spherical joints containing clearances in spatial multi-body systems was predicted based on the Archard wear model and multi-body system motion equations [20]. By considering different conditions, Zhuang [23] proposed a hybrid model for predicting the wear of a single revolute joint based on the Archard wear model, providing an idea for wear prediction under fluid lubrication. The analysis method based on the Archard wear model was also used in [6,25], in which, with parallel mechanisms as examples, the wear losses at the revolute joint and spherical joint clearances were calculated. It is not difficult to find that the calculation of wear prediction is primarily based on the Archard wear model, mainly because this model can be easily solved according to the standard contact force and slip distance. The Archard wear model is linear, and in studies on dynamics utilizing a continuous contact model to calculate contact collision force, it is very convenient to use such a mode to calculate wear depth. Reye's hypothesis wear model assumes that the work done by friction is proportional to the wear volume.

In contrast, the wear volume is inversely proportional to the shear stress between the contact bodies, so the wear loss between the contact bodies is calculated by the tangential contact force, which is the opposite of the process of calculating contact collision force by the normal contact force. Therefore, it is not commonly used. Moreover, the calculation of wear loss can also be obtained by the finite-element method, which can ensure high

calculation accuracy. However, considering the complexity of the mechanism and the difference in finite-element mesh division, the calculation cost and resources are difficult to guarantee, so the use of the finite-element method is still limited to a certain extent [30].

2.2.1. Wear Model

In the case of the spherical joint with clearance, wear would occur when the ball and shell are in contact and undergo relative motion. The Archard wear model is as follows [31]:

$$V = K_W \frac{F_N S}{H} \tag{10}$$

V is the wear volume, K_W is the dimensionless wear coefficient, F_N is the contact force, S is the relative slippage distance of the contact surface, and H is the hardness of the materials. In order to simplify the calculation, wear depth is usually instead of wear volume so that the above formula can be written as follows:

$$h_W = K_W \frac{F_N S}{HA} = \frac{k F_N S}{A} \tag{11}$$

where h_W represents the wear depth, A represents the contact area, and k is defined as the linear wear coefficient, which can be found in [32].

2.2.2. Wear Prediction of Spherical Joint Clearances

To investigate the influence of coatings and clearances on wear, polytetrafluoroethylene (PTFE) was selected as the coating material. Based on previous analysis and research of the dynamics of the mechanism containing spherical joint clearances, the wear losses of the mechanism with spherical joint clearances at different positions and with varying quantities with and without coatings were calculated. The contact force model and dynamic calculation method for the selected spherical joint clearances are the same as in [26]. The geometric parameters in the initial stage of dynamic analysis are corrected by calculating the wear depth. The corrected geometric model is then substituted into the dynamic calculation process to determine the contact state in the next step. This cycle continues until the simulation is completed. The specific analysis and calculation process is shown in Figure 5.
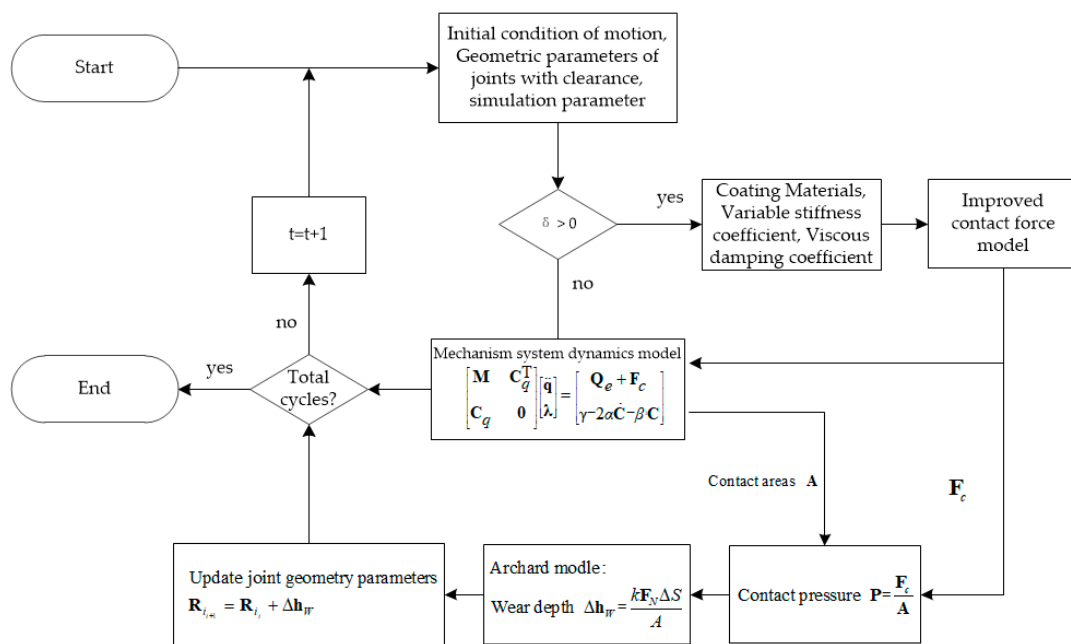

Figure 5. Wear prediction of spherical joints with clearance.

3. Design of Experimental Platform Containing Spherical Joint Clearances

With the continuous development of agricultural mechanization in China, the research and testing of agricultural machinery and equipment according to the requirements of intelligent and refined operations have attracted the attention of many scholars [33–36]. It is imperative to conduct studies on the automation and intelligence of small agricultural machinery in western hilly areas [2,37]. To solve the problems of high loss rate, crushing rate, and impurity rate during the harvesting operation of soybean combined harvesters [38], the research and development team of the author carried out research on the problems with many soybean picking machines; it is difficult to adapt them to diverse terrains, and they have a short working life and high loss rate [33,39–41]. At the same time, the development and testing of the prototype were started simultaneously, and the prototype model for this stage is shown in Figure 6a. The initial model design includes soybean picking, threshing, and sorting. Considering the precision of action control during the entire machine operation and the convenience of subsequent component maintenance, for the scissor action of the picking part, we planned to use the spatial linkage mechanism, as shown in Figure 6b, as the driving component. To evaluate the dynamic performance of this component under long-term operation, a spatial crank slider mechanism (RSSP), including spherical joint clearances and coatings was built, as shown in Figure 6c. The size of each rod in the model was proportional to the size of the original driving component. As for the overall structural design of the experimental platform and the machining and assembly of various components, consideration should be made in the following aspects: (i) Consider the interchangeability requirements of ideal joints and clearance joints, and the dimensions of the experimental platform and its components should be easy for disassembly and operation. (ii) The driving rod and connecting rod are homogeneous rods. Considering the influence of the inertial force of the components on the reaction force of the ideal spherical joints, to reduce the inherent error of the experimental platform, the balance mass blocks are added at both ends of the driving rod and connecting rod, so that the center of mass of each component will be maximally close to the geometric center. (iii) Limited by the experimental conditions, the rotating joint clearances are not considered in the experimental platform, so the rolling bearings are chosen as the rotating joints of the driving rod. The outer surface of the sphere and the inner surface of the shell of the two spherical joints are polished by sanding and polishing, and there are no requirements for the surface roughness of the remaining parts. (iv) The outer diameter of the sphere of ideal spherical joints is equal to the shell's inner diameter. In contrast, the difference between the outer diameter of the sphere of spherical joints containing clearances and the shell's inner diameter is 0.25 mm. Before adding a coating to the inner surface of the shell of the spherical joints containing clearances, it must be polished multiple times to ensure that its inner diameter is 0.08~0.12 mm smaller than the inner diameter of the shell of the ideal spherical joints.
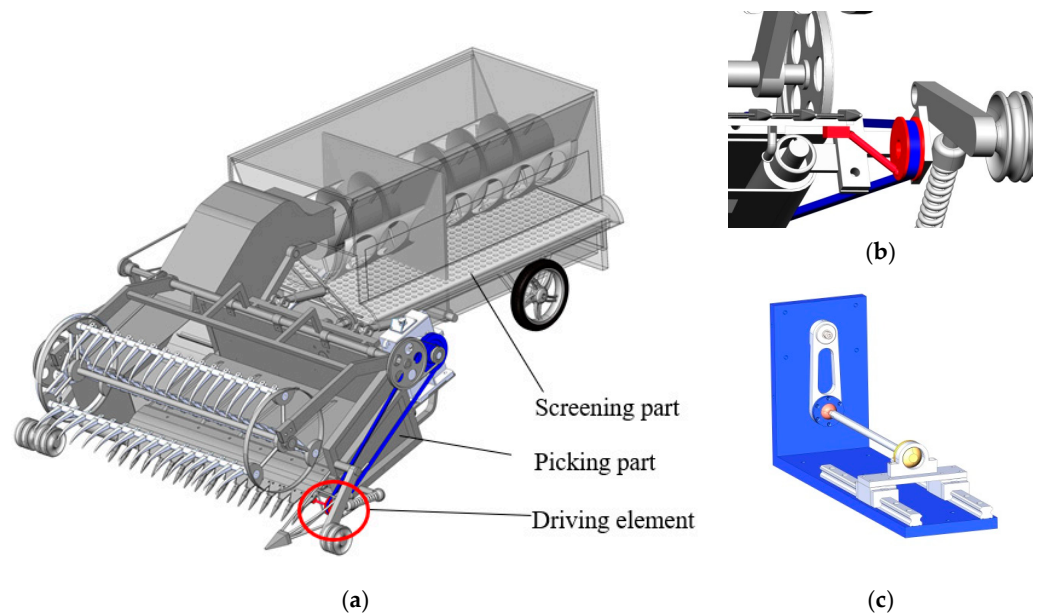
Figure 6. The design of the experimental platform. (**a**) Picking and sorting device for soybean. (**b**) Driving element. (**c**) Model building.

4. Experimental Equipment and Process

4.1. Experimental Equipment

This experiment mainly aims to measure the dynamic characteristics of a mechanism of spherical joints containing clearances with and without coatings. The structure and functional design of the experimental platform should be simple and easy to operate, integrating the spatial four-bar mechanism to be measured with the control system and measurement system. To reduce the impact of platform vibration caused by the motor driving the experimental platform, symmetrically distributed mass blocks are installed in the internal space of the experimental platform. For the convenience of disassembling and replacing spherical joints, the spherical joints and the rod are bolted together in the design. The two sets of spherical joints in the mechanism are the ideal and spherical joints containing clearances with specific positions marked in Figure 7. There is a 0.25 mm clearance between the shell and the sphere in the spherical joints containing clearances. In order to evaluate the effect of coatings on the dynamics of the mechanism containing clearances, additional spherical joints need to be produced, and the shell should be pre-treated and sprayed. Due to the specific preparation process, the coating thickness was about 0.1 mm. The particular production and coating preparation was entrusted to Kunshan Julin Machinery in Jiangsu Province of China. The resulting dynamic performance testing platform is shown in Figure 7. In the experiment, the displacement, velocity, and acceleration changes of the slider mass center with and without coatings in the clearances between the spherical joints were measured and calculated using a draw-wire displacement sensor and a built-in acceleration sensor located at the center of mass of the slider. In order to reduce the cumulative error during the experiment, all spherical joints are in a stable wear stage. Three sets of spherical joints should be selected to obtain the dynamic results of the slider under the same experimental scheme, and the results of the three measurements should be averaged as the final result. According to previous theoretical research, considering the sudden acceleration change at the starting point of the mechanism motion, some bad points of the measured slider during crank start and stop should be removed.
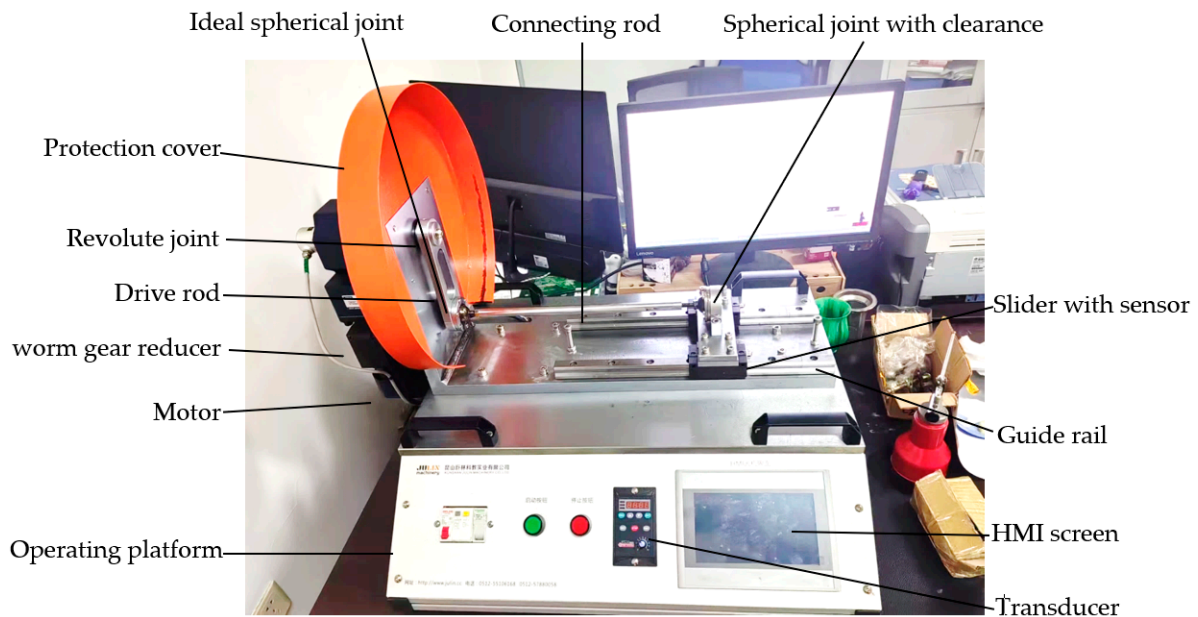
Figure 7. The experimental platform.

The experimental platform consists of two parts: the part above the platform (including the mechanism and testing equipment) and the part below the platform (including the driving rod (crank), connecting rod, slider, and parallel guide rail of the spatial four-bar mechanism). The deep groove ball bearing and grease lubrication are used to rotate the driving rod. The crank is connected to the frame, and the connecting rod is connected to the slider through ideal spherical joints and the spherical joints containing clearances, respectively. The length of the parallel guide rail is 1.5 times the maximum sliding distance. The motor and bevel gear reducer are installed on the back side of the crankshaft. The driving rod is driven by a stepper motor and outputs torque through a worm gear reducer. The spindle is equipped with a photoelectric sensor PX1, and the spindle speed is displayed in the frequency converter, as shown in the diagram.

In order to reduce relevant risks during the experimental process, a circular protective cover is installed on the crankshaft side, and the crankshaft speed should not exceed 110 r/min. Under the experimental platform are air switches, start/stop switches, frequency converters, and human–computer interaction interfaces. The human–computer interaction interface is shown in Figure 7, which includes the "start button", "stop button", "real-time curve", "zero position", and "reset button", of which the Start, Stop, and Reset functions are the same as external buttons. The speed control knob can set the driving speed, while the displacement, speed, and acceleration of the slider can be detected by replacing different sensors at the bottom of the slider.

Limited by the experimental conditions, this experiment mainly evaluates the acceleration changes at the slider's center of mass and the wear of the shell in the spherical joints containing clearances when the spindle speed is 60 r/min, the spherical joint clearance is 0.25 mm, and the coating thickness is 0.1 mm. The spherical joint containing clearances has dry friction, and other joints are fluid-lubricated. The clearance and wear of the rotating and moving joints are not considered in this experiment. The wear depth of the spherical joints with clearances and coatings was measured using a 3D contour measuring instrument. The measurement process is demonstrated in Figure 8, and the model and parameters of each equipment on the experimental platform are shown in Table 2. The test samples were two groups of six, including three uncoated spherical shells and three coated spherical shells with a coating thickness of 0.1 mm. Before testing, the samples

should be cleaned, and decontamination should be treated to prevent bumping during transport. In order to reduce the difficulty of the experiment, compared with the theoretical calculation results, the wear range of the spherical joint around the X-axis was about 360°. The 3D profile measuring instrument was selected to measure the surface profile of the shell within the unit square millimeter of every 90° rotation, and the maximum wear depth was selected. Considering the randomness of clearance and wear, this part must measure the three samples several times to obtain the maximum value. The measurement result takes two significant digits.
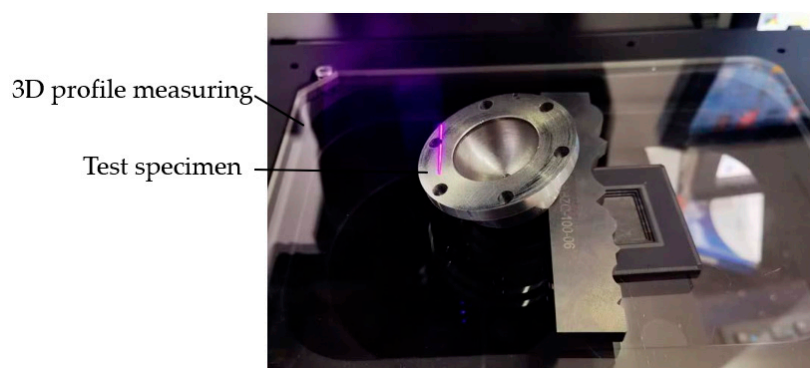
Figure 8. The measurement of wear depth.

Table 2. Equipment for the experiment platform.

Name	Model/Parameter
Variable-speed motor	100YT200GV22/1420 rpm
Displayer	TPC7032Ki
MAIN	DZ47sLE-C10
Photoelectric sensor (PX1)	K38-T3N1024B8/DPI: 1000P/R
Displacement sensor	MPS-M-2500mm-V1
Acceleration sensor	DYTRAN-3097A2/50 g
CPU	Intel Core i5-8500 CPU@3.00 GHZ
Helical gear reducer	100GF6RC/1:16
3D profilometer	VJ1010S

4.2. Coating Material and Preparation

Solid lubricants have the advantages of low evaporation rates, a wide range of working temperatures, radiation resistance, and corrosion resistance, which have been widely used in space mechanical lubrication [42,43], and such lubricants are very advantageous for mechanisms considering duration of space operation and accuracy of component motion. According to the previous discussion, the selection of coating materials must be based on the required dynamic characteristics of the mechanism and different materials should be selected to achieve vibration reduction and wear reduction while also meeting the requirements of load-bearing capacity, high-temperature characteristics, and oxidation resistance for coatings under various working conditions. Therefore, selecting coating materials is very important in coating design [41]. The solid lubricating materials commonly used in mechanical systems include five categories: polymers, layered structures, inorganic compounds, composite materials, and metals. The widely used materials and their advantages and disadvantages are shown in Table 3.

Table 3. Classification and characteristics of solid lubricating materials.

Name	Examples	Characteristic
Layered structure	MoS_2, WS_2, $NbSe_2$, Graphite	Strong loading capacity. Small friction coefficient and wear rate. Good lubrication performance.
Soft metal	Lead, Gold, Silver, Tin	Strong viscosity. Good wear resistance and lubrication properties.
High-molecular polymer	PTFE, PF, EP, PU	Polymers are generally suitable in toughness, do not damage the dual material, and can effectively absorb vibration without noise. Good low-temperature performance, even in a vacuum, can still play its lubrication role; Good chemical stability, friction, and wear on the atmosphere of the dependence is small.
Inorganic compound	ZnO, PbO, B_2O_3, SiO_2, MoO_3, metal fluoride such as BaF_2, GaF_2	High-temperature lubrication performance is good, and The antioxidant capacity is high at high temperatures.
Self-lubrication composites	Gather multiple materials together.	Low friction coefficient, long service life, and High reliability. There are not many varieties, and they are still to be developed.

The selection of coating materials in the mechanism joints containing clearances depends on the system's speed, external load, and actual operating conditions. Our experimental study mainly considers applying coatings at the joints containing clearances to achieve vibration reduction. Moreover, to meet the typical operation requirements of the experimental platform with coatings, the coating material should also have good lubrication properties. At the same time, to prevent relative slip between the coating and the substrate material, the selected coating material also needs to present good adhesion during the coating preparation process. PTFE (polytetrafluoroethylene) is an excellent anti-wear and self-lubricating material with outstanding wear resistance, low friction coefficient, and thermal stability, which can improve the self-lubricating and anti-wear properties of metal surfaces. Therefore, in our work, the PTFE polymer is used as the coating material to test the dynamic performance of the mechanism containing both coatings and clearances while ensuring the lubrication and adhesion of the spherical joint coating. The test results are compared with the numerical simulation results to verify the effects of joint clearances on the mechanism dynamics and the effectiveness of coatings in reducing system vibration, as discussed above. The structure of the spherical joints containing clearances is shown in Figure 9a, and the comparison before and after applying coatings to the inner surface of the shell is shown in Figure 9b.
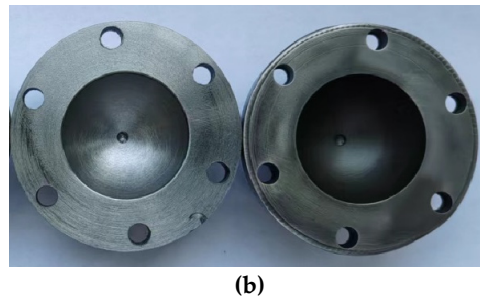

(a)

Figure 9. *Cont.*

(b)

Figure 9. Test structure and coating of spherical joint. (**a**) Spherical joint structure. (**b**) Coating in shell.

4.3. Experimental Design

According to different materials, thicknesses, and preparation processes, the coating has various effects on the joint and system dynamics of the clearance mechanism [25,26]. To reduce the difficulty of the experiment, discussions and experimental studies on the selection of different coating materials and coating preparation processes will not be considered in our work. Polytetrafluoroethylene (PEFT) will be used as the coating material in this study, with a coating thickness of 0.1 mm. According to previous research on the influence of coatings on the dynamics of the mechanism, the advantages of coatings over fluid lubrication in the mechanism can help address various issues caused by clearances, such as system vibration, reduced execution accuracy, and shortened service life. To verify this conclusion, the dynamic changes in the actuator when there are clearances and coatings in a single spherical joint in the four-bar linkage mechanism are evaluated in the experiment. The specific experimental scheme is shown in Table 4. When the machining size error between the inner diameter of the shell and the outer diameter of the sphere is minimal, the resulting clearance between the spherical joints is generally less than 0.01 mm [44]. The spherical joints with small clearances can be considered ideal in this case.

Table 4. The experimental test design.

No.	Actuating Speed (rpm)	Clearance (mm)	Coating
1	60	Ideal clearance 0.002	No
2	60	Spherical joint with clearance 0.25	No
3	60	Spherical joint with clearance 0.25	PTFE

4.4. Experimental Results

Various members of the space four-bar mechanism are made of medium carbon steel, which is homogeneous, and the position of each member's mass center remains unchanged through balanced mass. Although the surface and joints of the rod have undergone finish machining and surface polishing, considering the assembly errors of various components of the experimental platform, the clearances between spherical joints, uneven coating thickness, and other issues, the displacement, velocity, and acceleration of the slider are measured by taking the average of multiple measurements. The displacement of the slider can be measured and read by a displacement sensor or directly displayed on the human–computer interaction interface. According to the theoretical analysis above, compared with the ideal spherical joints, the displacement of the system actuator under the influence of spherical joints containing clearances remains unchanged, and the velocity only shows small step-like changes. The main reason for the intense vibration of the system and decreased accuracy of the execution action is the sudden change in acceleration. Therefore, in order to accurately obtain the acceleration change of the slider during the

experiment, a DYTRAN-3097A2 three-axis acceleration sensor is installed below the slider for measurement, and data are sorted and stored through a working machine after each measurement is completed.

Numerical simulation was conducted for the space four-bar mechanism (RSSP), and the geometric dimensions of various components of the experimental platform are shown in Table 5. In the following three conditions—small clearances, big clearances, and clearances with coatings between spherical joints—the changes in displacement and velocity at the slider's center of mass over one cycle are compared with the experimental results, as shown in Figure 10. It can be seen that when there are clearances or clearances with coatings between spherical joints, under the interference from electrical signals and the natural frequency of components, the differences between the experimental results and the simulation results of the slider displacement and velocity are minimal. If the effects of cumulative error (e.g., the vibration of the experimental platform and the interference of data signals) are not considered, the displacement and velocity changes of the slider can be regarded as consistent with the numerical simulation results. This conclusion is consistent with the previous conclusion that the spherical joints containing clearances have a relatively small impact on the displacement and velocity of the system actuator. It should be noted that when there are clearances and coatings between spherical joints, the fluctuation of the slider speed is slightly smoother compared to the ideal spherical joints and to when only clearances (without coatings) are considered for the spherical joints, which is consistent with the conclusion of numerical simulation.

Table 5. The geometric parameters of the component in the mechanism systems.

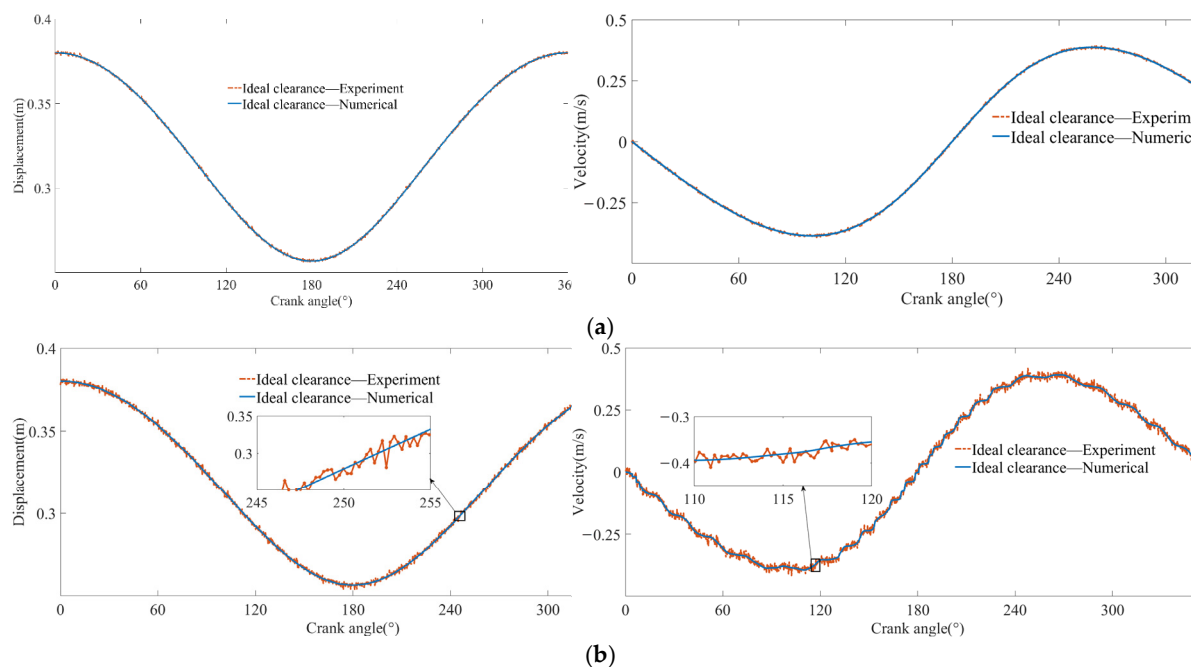| Name	Symbol	Length (m)	Mass (kg)
Crank	L_1	0.14	1.3
Connecting rod	L_2	0.38	1.2
Slider	L_3	-	2.2

Figure 10. *Cont.*
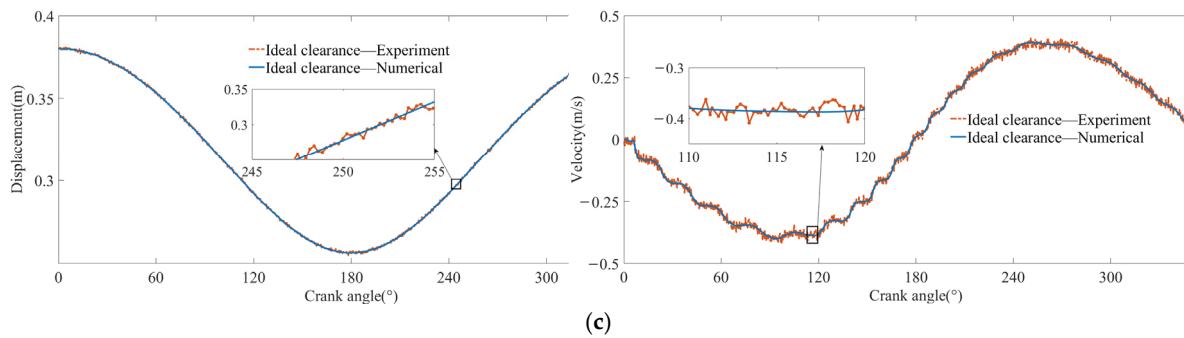
(c)

Figure 10. Displacement and velocity of the slider in different schemes. (**a**) Scheme 1. (**b**) Scheme 2. (**c**) Scheme 3.

4.4.1. Slider Acceleration

As the end actuator of the space four-bar mechanism, the acceleration change of the slider can best reflect the dynamic performance of the mechanism. In order to verify the previous conclusion about the influence of clearances and coatings of spherical joints on the dynamic performance of the mechanism, the ideal spherical joints at the connection between the slider and the connecting rod are replaced with spherical joints with big clearances but no coatings and spherical joints with big clearances and coating. Similarly, the method used to evaluate the dynamic performance of the mechanism when there are clearances in spherical joints is used for numerical simulation. The simulation parameters are shown in Table 6. For the following three types of spherical joints—spherical joints with ideal clearance, spherical joints with clearance of 0.25 mm, and spherical joints with clearance of 0.25 mm and coatings—the changes in acceleration at the slider's center of mass are compared with the comparison results shown in Figures 11 and 12, respectively.

Table 6. Simulation parameters.

Name	Value	Name	Value
Recovery coefficient c_r	0.46	Angular velocity rpm	60
The radius of sphere/mm	15	Inner radius of sphere/mm	15.5
Elastic modulus of the base Gpa	207	Elastic modulus of coating Gpa	2.86
Poisson's ratio of the base	0.3	Poisson's ratio of coating	0.4
Dynamic friction coefficient u_d	0.01	The dynamic friction coefficient of the coating	0.167
Initial step size	1×10^{-5}	Coating thickness l_c/mm	0.1
Min step size	1×10^{-7}	Base thickness l_s/mm	3.9
Baumgarte α, β	5		

According to Figure 11, when the clearance between the spherical joints is ideal, the acceleration change of the slider is affected by the reaction force of the joint. The acceleration is a continuous non-zero curve except for the start and end positions. When the spherical joints contain clearances, the numerical solution of the slider acceleration exhibits intermittent abrupt changes, with some positions showing zero acceleration. However, the overall change trend is consistent with the numerical results for the spherical joints containing ideal clearance. This is mainly because the sphere is instantly in a free state during contact and collision and is not subjected to external forces, resulting in 0 acceleration. Compared with the numerical results for spherical joints containing clearances, zero acceleration was not detected in the experiment. Considering the accumulation of various errors and signal interference during the experiment, the overall change trend of the acceleration experimental results at the slider's center of mass can be regarded as consistent with the numerical results. Therefore, the acceleration test results of the slider

can prove the correctness of the contact force model proposed earlier for the spherical joints with clearances, as well as the conclusions about the influence of the spherical joint clearances on the dynamics of the mechanism. When considering both clearances and coatings for the spherical joints, the acceleration change curve at the slider's center of mass in a single cycle is shown in Figure 12, and the enlarged acceleration curve of the slider when the crank rotates to the range of 120~240° is shown in Figure 12b. When there are clearances and coatings in the spherical joints, the overall trend of the acceleration change at the slider's center of mass is consistent with that of the spherical joints containing ideal clearances. The amplitude is slightly reduced compared with the numerical results of spherical joints with clearances and no coatings. Considering the effects of various errors during the experiment [25], the experimental results can be regarded as consistent with the numerical results.
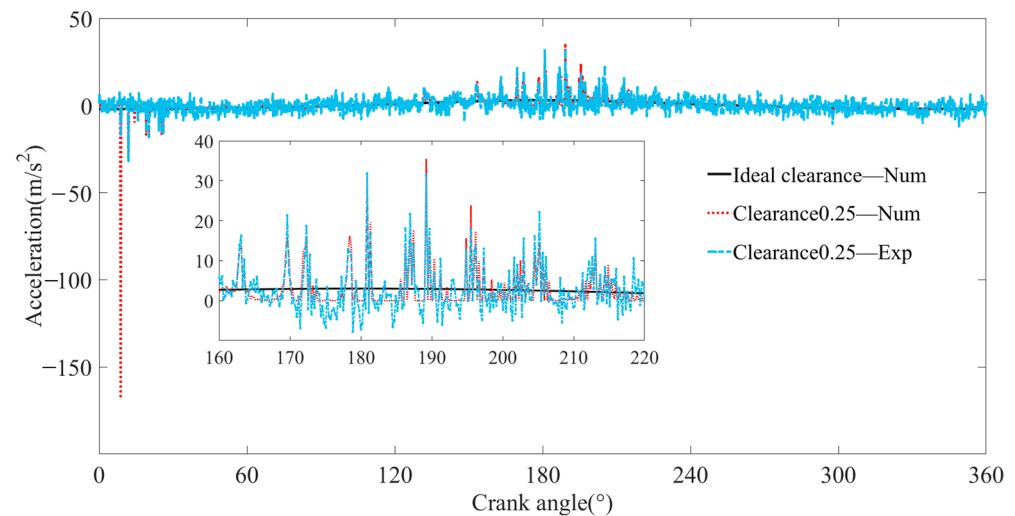
Figure 11. Acceleration of the rocker with clearance and no coating.
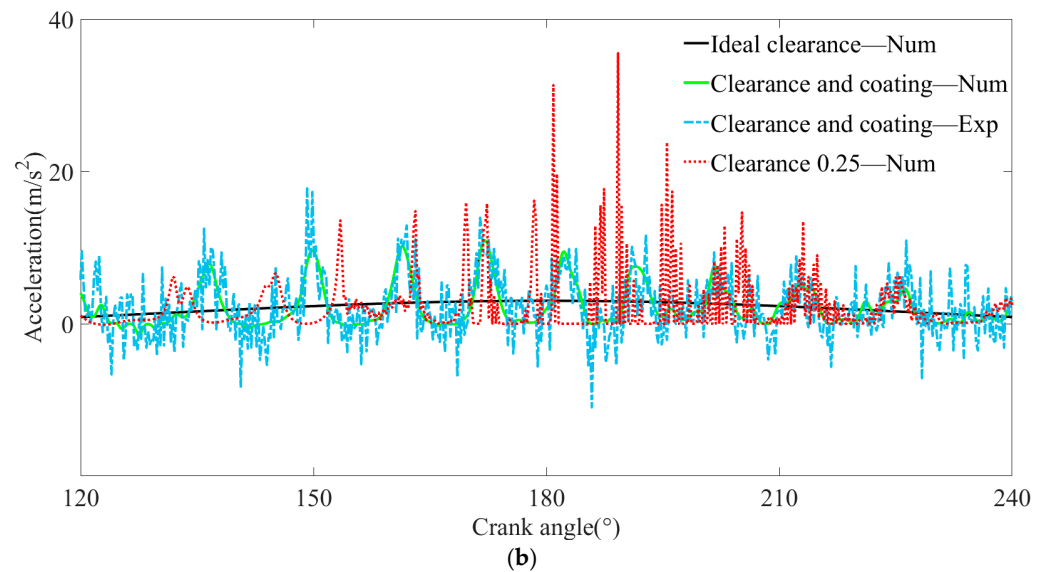

(a)
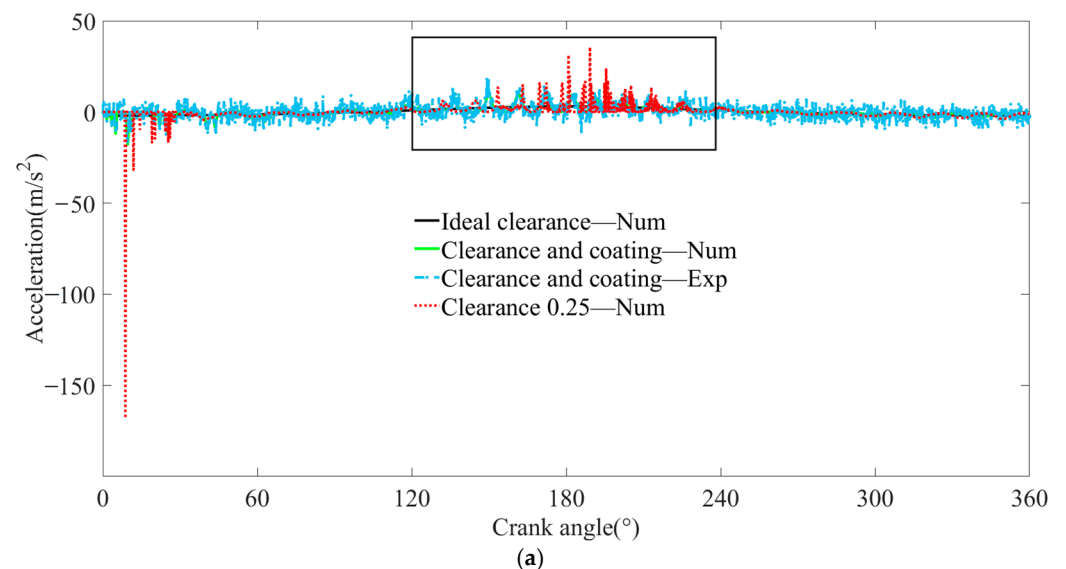
Figure 12. *Cont*.

Figure 12. Acceleration of the slider with clearance and coating. (**a**) Crank angle 0~360°. (**b**) Crank angle 120~240°.

The specific experimental and numerical results of slider acceleration are shown in Table 7. The following can be seen: (i) In both schemes, the experimental results of all parameters are more significant than corresponding numerical solutions, which is due to various factors such as component machining accuracy, assembly error, additional dynamic load, measurement error, etc. (ii) According to the experimental results, it can be seen that applying coatings to the clearances between the spherical joints can effectively reduce the abrupt change in slider acceleration caused by the clearances. The maximum, minimum, and mean amplitude are reduced by 58.46%, 88.63%, and 4.86%, respectively. Numerical discretization is described by the mean square error, which is decreased by 57.89% overall. (iii) The average amplitude of the numerical solution, when coatings are applied to the spherical joint clearances, is slightly higher than that without coatings. This is mainly because the vibration amplitude is reduced after adding coatings, but it will increase the vibration frequency. The experimental results did not reflect this attribute due to limited measurement accuracy. The average amplitude of the experimental results with coatings applied to the clearances between the spherical joints is lower than without coatings.

Table 7. Acceleration of slider in different schemes.

No.	Max (m/s^2)	Min (m/s^2)	Amplitude (m/s^2)	MSE (m/s^2)^2
2-Numerical	35.5464	−168.2078	1.6519	27.5622
2-Experimental	38.4330	−165.0061	3.1863	36.0878
3-Numerical	10.9478	−17.8676	1.7173	7.2335
3-Experimental	15.9639	−18.7684	3.0315	15.1965

4.4.2. Wear of Spherical Joints Containing Clearances

After verifying that the simulation results of the effects of spherical joint clearances on system dynamics are consistent with the experimental results, the spherical joint clearance of 0.25 mm without coating and the spherical joint clearance of 0.25 mm after adding a layer of 0.1 mm were selected as the research objects. After preliminary running-in and pre-heat treatment, the two types of spherical joints were placed in a four-bar mechanism with completely identical working conditions for wear experiments, with a driving speed of 60 rpm and running hours of 7.5 h. Lubricating grease and lubricating oil were added to the ideal spherical joints and guide rail for lubrication. According to the dynamic simulation

results of the mechanism under the influence of spherical joint clearances in reference [29], the space crank slider mechanism is shown in Figure 7. The wear of the spherical joints containing clearances is mainly manifested in the rotation area around the x-axis, so in order to reduce the difficulty of the experiment, we measured the circumferential wear depth at the connecting position of the shell after the two types of spherical joints were worn. Considering that the wear range of the spherical joints around the x-axis is about 360°, a 3D contour measuring instrument was used to measure the surface contour of the shell within a unit square millimeter range for rotation of every 90°. The maximum wear depth was selected, and considering the randomness of clearance and wear, this part needed to be determined through multiple measurements. Table 8 shows the maximum wear depth and corresponding measurement contours and lines selected after numerous measurements of the two types of spherical joints in four areas of the entire circumference. It can be seen that within the range of 180~270° around the x-axis of the spherical joints, the maximum wear depth in the wear area for spherical joint clearance with coating is higher than that without coating.

In contrast, the maximum wear depth in other wear areas decreases compared to the joint without coating. This is mainly due to the randomness in the contact collision process and the cumulative error in the experimental method. The average of the other three sets of measurement values can be used as a substitute for parameter comparison in the later stage. The completeness and reliability of experimental data will be gradually improved in our future research work. Similarly, the system dynamics calculation and wear prediction methods for the mechanism containing spherical joint clearances and coatings are adopted to predict the wear depths when the spherical joint clearances are with and without coatings, with the prediction results shown in Figures 13a and 13b, respectively. It can be seen that when the clearance between the spherical joints is 0.25 mm, adding coating can reduce the maximum wear depth on the inner surface of the shell, which is consistent with the prediction of spherical joint wear when the spherical joint clearance is 0.5 mm in [29].

As can be seen from Table 9, the numerical solution of the mechanism system dynamics with clearance of spherical joints is smaller than the test results. The main reasons for the error include the following: (i) The theoretical model used in numerical simulation does not consider the clearance of other joints, and the joints used in the mechanism system used in the experimental platform all have specific clearances. (ii) The cumulative error caused by the measurement accuracy, equipment accuracy, machining accuracy and insufficient lubrication conditions in the experiment cannot be ignored. (iii) Due to the limited experimental conditions, the method of measuring the surface profile of the shell within the unit square millimeter by rotating the ball hinge at a certain angle and then selecting the maximum wear depth needs to be further demonstrated and optimized. However, the wear depth is on the order of one micron, and the change rule of the wear depth affected by the coating is the same, which can demonstrate the feasibility of the conclusion that the addition of coating on the clearance of the spherical joints can slow down the vibration of the mechanism system to a certain extent, and also verify the effectiveness of the addition of coating on the clearance joint to reduce the joint wear.
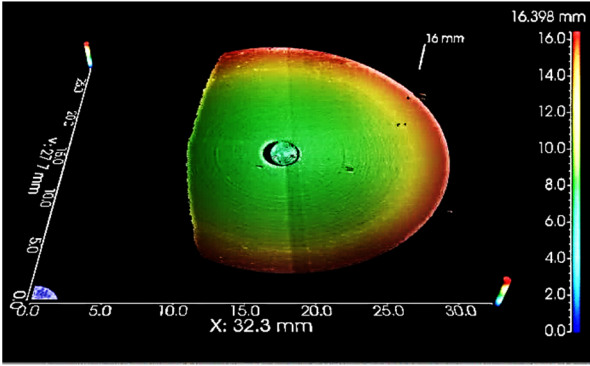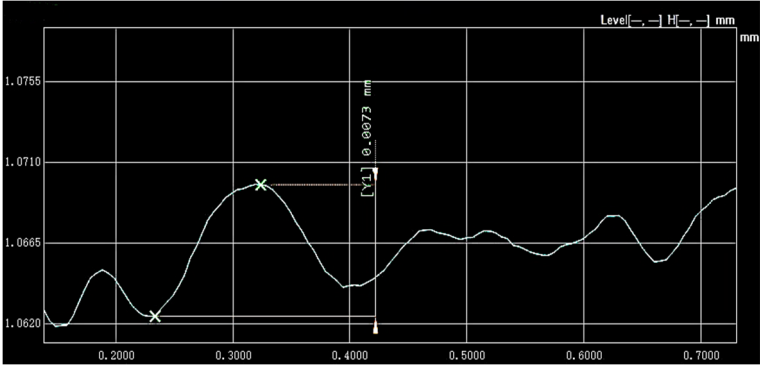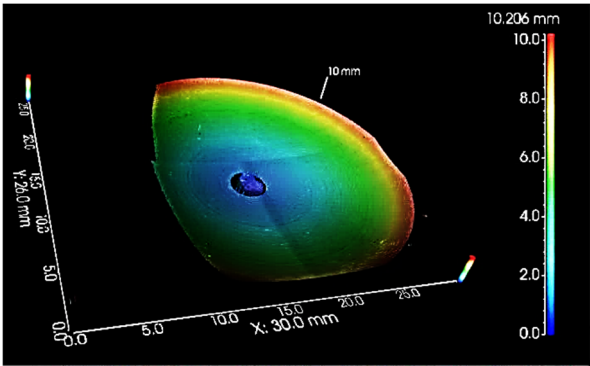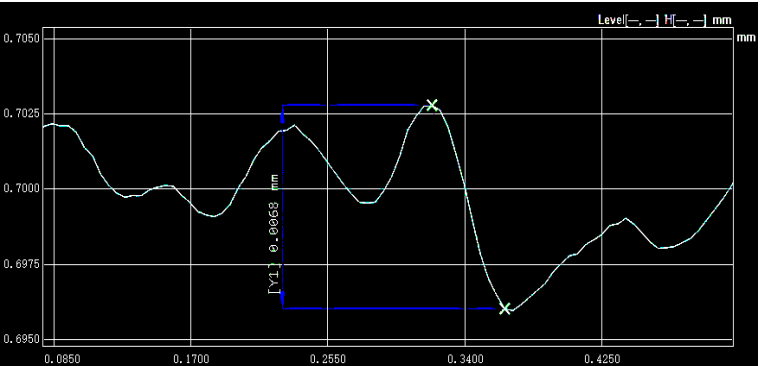
Table 8. The measurement of wear depth.

No.	Type	Wear Depth	3D Profile	Measure Curve
2	0~90°	0.0073 mm		
	90~180°	0.0068 mm		
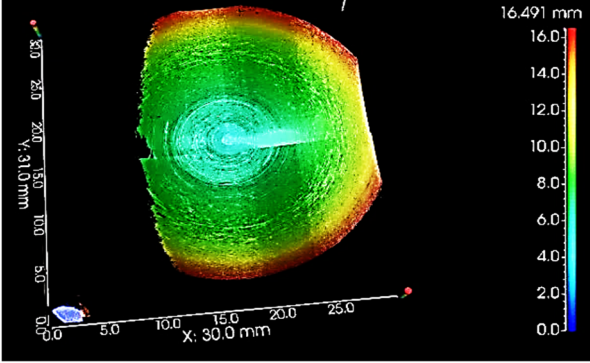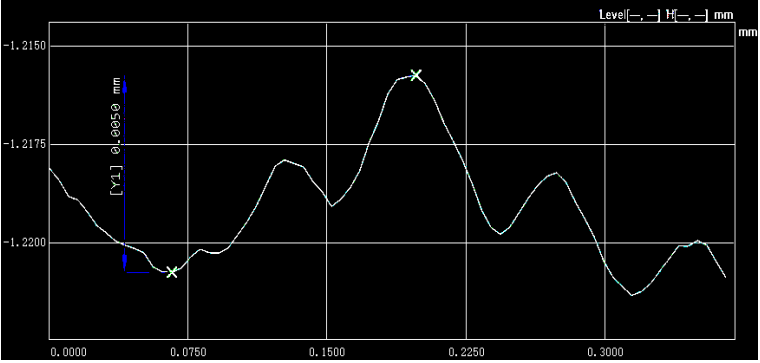
Table 8. *Cont.*

No.	Type	Wear Depth	3D Profile	Measure Curve
2	270~360°	0.0074 mm		
3	0~90°	0.0041 mm		

Table 8. *Cont.*

No.	Type	Wear Depth	3D Profile	Measure Curve
3	90~180°	0.0036 mm		
	180~270°	0.0074 mm		

Table 8. *Cont.*

No.	Type	Wear Depth	3D Profile	Measure Curve
3	270~360°	0.0050 mm		
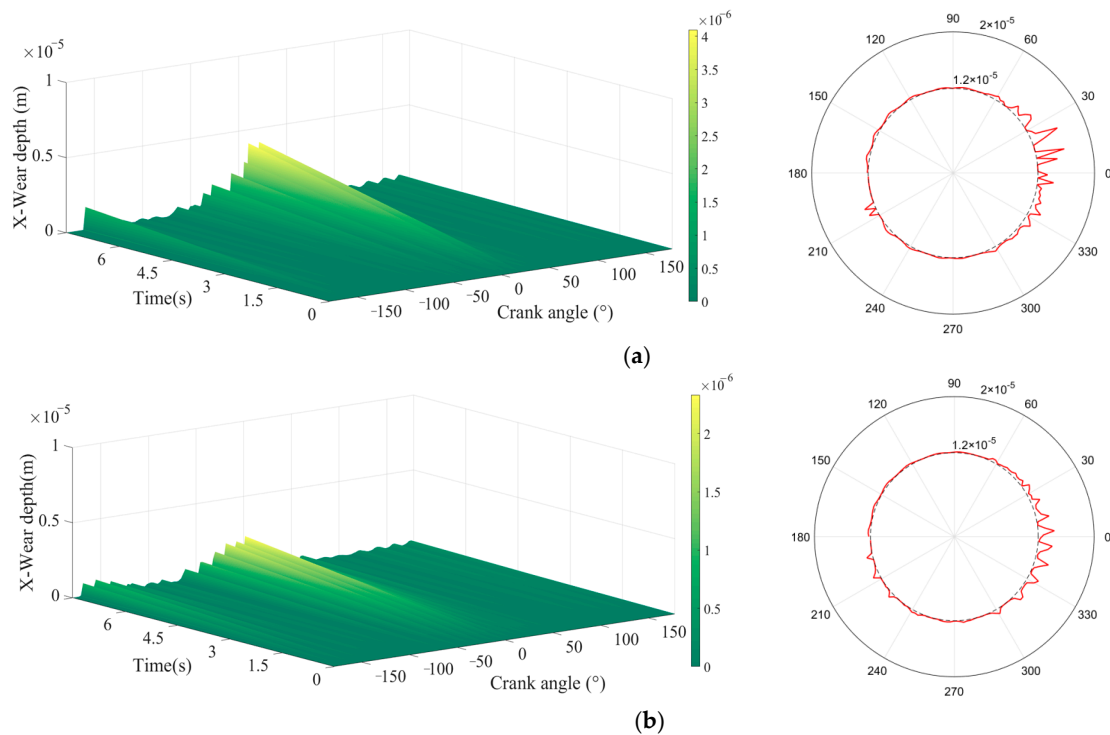
Figure 13. Wear prediction of spherical joints with clearance. (**a**) Spherical joint with clearance. (**b**) Spherical joint with clearance and coating.

Table 9. Wear prediction.

No.	Measuring Value (mm)	Simulation Value (mm)
2	7.3×10^{-3}	4.099×10^{-3}
2	6.8×10^{-3}	3.882×10^{-3}
2	6.3×10^{-3}	3.763×10^{-3}
2	7.4×10^{-3}	3.987×10^{-3}
3	4.1×10^{-3}	2.332×10^{-3}
3	3.6×10^{-3}	2.112×10^{-3}
3	4.2×10^{-3}	2.075×10^{-3}
3	5.0×10^{-3}	2.421×10^{-3}

5. Conclusions

Based on the previous theoretical research on the dynamics of the mechanism containing spherical joint clearances and coatings, the scissors part of the soybean picking and sorting machine developed by our project team was the research object of our study, and we also independently designed and built a space four-bar mechanism experimental platform. The influence of clearances on the dynamics of the mechanism is verified by comparing the dynamic calculation results of the effects of spherical joints containing big and small clearances on the actuator. On this basis, the coating was applied to the inner surface of the shell, and wear experiments were conducted on the spherical joints under the same working conditions. The wear depth in different areas of the worn surface of the shell was measured using a 3D profilometer, and the measurement results were compared with the predicted values. The research results indicate the following:

(1)　The experimental measurement results and the numerical simulation results of the actuator acceleration of the spatial four-bar mechanism considering spherical joint clearances show a consistent trend and amplitude of change, which verifies the previous conclusions about the influence of joints containing clearances on the dynamics of

the mechanism. At the same time, it can also prove the correctness of the calculation method for the mechanism dynamics considering the spherical joint clearances.

(2) The experimental results under the presence of both the spherical joints and the coatings show that the maximum wear depth without coating is 7.4×10^{-8} mm, and the maximum wear depth with the coating is 5.0×10^{-8} mm. The simulation results show that the maximum wear depth without coating is 4.099×10^{-3} mm, and the maximum wear depth with coating is 2.421×10^{-3} mm, and there are deviations under the same order of magnitude. However, the overall change law is consistent, which can verify the effectiveness of coating on joint wear reduction. There are deviations in the results of maximum wear depth under the same order of magnitude. Still, the overall change rule is consistent, which can verify the effectiveness of coating on joint wear reduction. Considering the cumulative impact of errors, the correctness of the mechanism system dynamics calculation method involving gap and coating in the literature [26,27] can be proved.

(3) The experiment evaluated the dynamics of the mechanism with the presence of joint clearances. The experimental platform design and experimental method considering the spherical joint clearances can provide the experimental basis for dealing with the contact collision problem of spherical joints. The conclusion that coatings can reduce the vibration amplitude of the mechanism and alleviate joint wear can provide an idea for the development of agricultural machinery towards precision and intelligence by considering joint lubrication and system vibration reduction.

References

1. Yan, S.Z.; Xiang, W.W.K.; Huang, T.Q. Advances in Modeling of Clearance Joints and Dynamics of Mechanical Systems with Clearances. *Acta Sci. Nat. Univ. Pekin.* **2016**, *4*, 741–756.
2. Zhao, C.J. Current situations and prospects of smart agriculture. *J. South China Agric. Univ.* **2021**, *42*, 1–7.
3. Flores, P.; Lankarani, H.M. Spatial rigid-multibody systems with lubricated spherical clearance joints: Modeling and simulation. *Nonlinear Dyn.* **2009**, *60*, 99–114. [CrossRef]
4. Flores, P.; Ambrósio, J.; Claro, J.C.P.; Lankarani, H.M. Dynamics of Multibody Systems with Spherical Clearance Joints. *J. Comput. Nonlinear Dyn.* **2006**, *1*, 240–247. [CrossRef]
5. Wang, G.X.; Liu, H.Z. Dynamics Analysis of 4-SPS/CU Parallel Mechanism with Spherical Joint Clearance. *J. Mech. Eng.* **2015**, *51*, 43–51. [CrossRef]
6. Hou, Y.L.; Deng, Y.J.; Zeng, D.X. Dynamic modelling and properties analysis of 3-RSR parallel mechanism considering spherical joint clearance and wear. *J. Cent. South Univ.* **2021**, *28*, 712–727. [CrossRef]

7. Tian, Q.; Zhang, Y.Q.; Chen, L.P.; Flores, P. Dynamics of spatial flexible multibody systems with clearance and lubricated spherical joints. *Comput. Struct.* **2009**, *87*, 913–929. [CrossRef]

8. Federico, J.; Cardona, A. Non-smooth model of a frictionless and dry three-dimensional revolute joint with clearance for multibody system dynamics. *Mech. Mach. Theory* **2018**, *121*, 335–354.

9. Marques, F.; Rychecký, D.; Isaac, F.; Hajžman, M.; Polach, P.; Flores, P. Spatial Revolute Joints with Clearance and Friction for Dynamic Analysis of Multibody Mechanical Systems. In Proceedings of the 4th Joint International Conference on Multibody System Dynamics, Montréal, QC, Canada, 29 May–2 June 2016.

10. Bai, Z.F.; Jiang, X.; Li, J.Y.; Zhao, J.J. Dynamic analysis of mechanical system considering radial and axial clearances in 3D revolute clearance joints. *J. Vib. Control* **2020**, *27*, 1893–1909. [CrossRef]

11. Akhadkar, N.; Acary, V.; Brogliato, B. 3D Revolute Joint with Clearance in Multibody Systems. *Comput. Kinemat.* **2018**, *50*, 11–18.

12. Wu, X.Z.; Sun, Y.; Wang, Y.; Chen, Y. Dynamic analysis of the double crank mechanism with a 3D translational clearance joint employing a variable stiffness contact force model. *Nonlinear Dyn.* **2019**, *99*, 1937–1958. [CrossRef]

13. Flores, P.; Ambrósio, J.; Lankarani, H.M. Contact-impact events with friction in multibody dynamics: Back to basics. *Mech. Mach. Theory* **2023**, *184*, 105305. [CrossRef]

14. Wang, G.X.; Jia, W.X.; Cheng, F.; Flores, P. An enhanced contact force model with accurate evaluation of the energy dissipation during contact-impact events in dynamical systems. *Appl. Math. Model.* **2024**, *135*, 51–72. [CrossRef]

15. Mukras, S.; Kim, N.H.; Sawyer, W.G. *Design Theory and Computational Modeling Tools for Systems with Wear*; Sae Technical Paper Series; SAE International: Warrendale, PA, USA, 2007; pp. 1–10. [CrossRef]

16. Mukras, S.; Mauntler, N.; Kim, N.H.; Schmitz, T.; Sawyer, W.G. (Eds.) Dynamic Modeling of a Slider-Crank Mechanism with Joint Wear. In Proceedings of the 32nd Annual Mechanism and Robotics Conference, New York, NY, USA, 3–6 August 2008; ASME: New York, NY, USA, 2008.

17. Mukras, S.; Kim, N.H.; Mauntler, N.A.; Schmitz, T.L.; Sawyer, W.G. Analysis of planar multibody systems with revolute joint wear. *Wear* **2010**, *268*, 643–652. [CrossRef]

18. Mukras, S.; Mauntler, N.A.; Kim, N.H.; Schmitz, T.L.; Sawyer, W.G. Modeling a Slider-Crank Mechanism with Joint Wear. *SAE Int. J. Passeng. Cars-Mech. Syst.* **2009**, *2*, 600–612. [CrossRef]

19. Flores, P. Modeling and simulation of wear in revolute clearance joints in multibody systems. *Mech. Mach. Theory* **2009**, *44*, 1211–1222. [CrossRef]

20. Wang, G.X.; Liu, H.Z.; Deng, P.S. Dynamics Analysis of Spatial Multibody System with Spherical Joint Wear. *J. Tribol.* **2015**, *137*, 021605. [CrossRef]

21. Wang, G.X.; Liu, H.Z. Three-Dimensional Wear Prediction of Four Degrees of Freedom Parallel Mechanism with Clearance Spherical Joint and Flexible Moving Platform. *J. Tribol.* **2018**, *140*, 021605. [CrossRef]

22. Wang, G.X.; Liu, H.Z.; Deng, P.S. Dynamic Analysis of 4-SPS/CU Parallel Mechanism Considering Three-Dimensional Wear of Spherical Joint with Clearance. *J. Tribol.* **2017**, *139*, 021608. [CrossRef]

23. Zhuang, X.C.; Sajad, S.A.; Yu, T.X.; Liang, X.H. A hybrid model for wear prediction of a single revolute joint considering a time-varying lubrication condition. *Wear* **2020**, *442–443*, 203124. [CrossRef]

24. Feng, K.; Smith, W.A.; Peng, Z.X. Use of an improved vibration-based updating methodology for gear wear prediction. *Eng. Fail. Anal.* **2021**, *120*, 105066. [CrossRef]

25. Li, Y.Y.; Yang, Y.; Li, M.; Liu, Y.F.; Huang, Y.F. Dynamics analysis and wear prediction of rigid-flexible coupling deployable solar array system with clearance joints considering solid lubrication. *Mech. Syst. Signal Process.* **2022**, *162*, 108059. [CrossRef]

26. Jing, Q.; Liu, H.Z. Dynamic analysis and wear calculation of space deployable mechanism considering spherical joints with clearance and coating. *Proc. Inst. Mech. Eng. Part C J. Mech. Eng. Sci.* **2023**, *237*, 2729–2752. [CrossRef]

27. Jing, Q.; Liu, H.Z. Dynamics and Wear Prediction of Mechanisms Considering Multiple Clearances and Coatings. *Lubricants* **2023**, *11*, 310. [CrossRef]

28. Jing, Q.; Liu, H.Z. Dynamic characteristics of linkage mechanism considering clearance of cylinder pair. *J. Vib. Shock* **2021**, *40*, 32–39.

29. Flores, P.; Machado, M.; Seabra, E.; Silva, M.T. A Parametric Study on the Baumgarte Stabilization Method for Forward Dynamics of Constrained Multibody Systems. *J. Comput. Nonlinear Dyn.* **2011**, *6*, 011019. [CrossRef]

30. Wang, G.; Liu, H. Research progress of joint effects model in multibody system dynamics. *Chin. J. Oftheoretical Appl. Mech.* **2015**, *47*, 31–50. [CrossRef]

31. Archard, J.F. Contact and Rubbing of Flat Surfaces. *J. Appl. Phys.* **1953**, *24*, 981–988. [CrossRef]

32. Yang, L.J. A test methodology for the determination of wear coefficient. *Wear* **2005**, *295*, 1453–1461. [CrossRef]

33. Zhou, Y.J.; Luo, B.; Liu, D.W.; Liu, D.; Qiu, Y.; Zhou, Y. Design and experiment of rape cutter in 4LZ-4.0 grain combine harvester. *J. Chin. Agric. Mech.* **2023**, *44*, 22–27.

34. Zhang, S.C.; Wei, X.H.; Deng, Y.; Qi, C.Q.; Ji, X.; Wang, A.Z. Design and experiments of the whole field path trackingalgorithm for a trackbased harvester. *Trans. Chin. Soc. Agric. Eng.* **2023**, *39*, 36–45.

35. Liu, J.J.; Ma, L.; Xiang, W.; Yan, B.; Wen, Q.H. Design and test of the header structure of 4QM-0 fiber corps green forage combine harvester. *J. Chin. Agric. Mech.* **2022**, *43*, 20–25.

36. Lian, G.D.; Wei, X.X.; Ma, L.N.; Zhou, G.H.; Zong, W.Y. Design and experiments of the axial-flow spiral drum threshing device for the edible sunflower. *Trans. Chin. Soc. Agric. Eng.* **2022**, *38*, 42–50.

37. Du, Y.F.; Fu, S.H.; Mao, E.R.; Zhu, Z.X.; Li, Z. Development Situation and Prospects of Intelligent Design for Agricultural Machinery. *Trans. Chin. Soc. Agric. Mach.* **2019**, *50*, 1–17.

38. Jin, C.Q.; Guo, F.Y.; Xu, J.S.; Li, Q.L.; Chen, M.; Li, J.J.; Yin, X. Optimization of working parameters of soybean combine harvester. *Trans. Chin. Soc. Agric. Eng.* **2019**, *35*, 10–22.

39. Luo, H.B.; Wang, J.J.; Lian, X.; Geng, B.L.; Li, F. Design and experiment of small narrow range segmented harvester hilly area. *Agrucultural Res. Arid. Areas* **2024**, *9*, 86–88.

40. Lian, X.; Wang, J.J.; Zhu, Y. Research status analysis of key technology and loss of soybean harvester header. *J. Chin. Agric. Mech.* **2024**, *45*, 8.

41. Yang, J.H.; Cui, M.; Guo, M.; Zhao, Y.P.; Ni, G.Q. Development strategy and thinking of harvester product technology using soybean and corn interplanting mode. *Farm Mach.* **2024**, *5*, 283–293.

42. Sun, R.L.; Sun, S.W.; Guo, L.X.; Yang, D.Z. Application of Solid Lubrication Technique for Space Mechanism. *Aerosp. Mater. Technol.* **1999**, *29*, 1–6.

43. Ma, G.Z.; Xu, B.S.; Wang, H.D.; Si, H.J. State of Research on Space Solid Lubrication Materials. *Mater. Rep.* **2010**, *24*, 68–71.

44. Flores, P.; Koshy, C.S.; Lankarani, H.M.; Ambrósio, J.; Claro, J.C.P. Numerical and experimental investigation on multibody systems with revolute clearance joints. *Nonlinear Dyn.* **2010**, *65*, 383–398. [CrossRef]